This is a repository copy of *MiR-29 coordinates age-dependent plasticity brakes in the adult visual cortex*.

White Rose Research Online URL for this paper:
http://eprints.whiterose.ac.uk/166619/

Version: Accepted Version

MiR-29 coordinates age-dependent plasticity brakes in the adult visual cortex

Debora Napoli[1,2], Leonardo Lupori[1], Raffaele Mazziotti[7], Giulia Sagona[2,7], Sara Bagnoli[1], Siwei Chen[5], Erika Kelmer Sacramento[4], Johanna Kirkpartick[4], Christophe Magnan[5], Alessandro Ori[4], Elena Putignano[2], Muntaha Samad[5], Eva Terzibasi Tozzini[1], Paola Tognini[1,9], Pierre Baldi[5], Jessica C.F. Kwok[3,8], Alessandro Cellerino[1,4], Tommaso Pizzorusso[1,2,7]

1. BIO@SNS lab, Scuola Normale Superiore, Pisa, Italy.
2. Institute of Neuroscience, National Research Council, Pisa, Italy.
3. School of Biomedical Sciences, University of Leeds, Leeds, UK.
4. Leibniz Institute on Aging – Fritz Lipmann Institute (FLI), Jena, Germany.
5. Institute for Genomics and Bioinformatics, School of Information and Computer Sciences, University of California, Irvine, CA, USA.
6. Department of Clinical and Experimental Medicine, University of Pisa; Department of Developmental Neuroscience, IRCCS Stella Maris Foundation, Pisa, Italy.
7. Department of Neuroscience, Psychology, Drug Research and Child Health NEUROFARBA University of Florence, Area San Salvi - Pad. 26, Florence, Italy.
8. Institute of Experimental Medicine, Czech Academy of Science, Prague, Czechia.
9. Department of Translational Research and New Technologies in Medicine and Surgery, University of Pisa, Pisa, Italy

Abstract

Visual cortical circuits show profound plasticity during early life and are later stabilized by molecular "brakes" limiting excessive circuit rewiring beyond a critical period. How the appearance of these factors is coordinated during the transition from development to adulthood remains unknown. We analyzed the role of miR-29a, a miRNA targeting factors involved in several important pathways for plasticity such as extracellular matrix and chromatin regulation. We found that visual cortical miR-29a expression in the visual cortex dramatically increases with age, but it is not experience-dependent. Precocious high levels of miR-29a induced by targeted intracortical injections of a miR-29a mimic blocked ocular dominance plasticity and caused an early appearance of perineuronal nets. Conversely, inhibition of miR-29a in adult mice using LNA antagomirs activated ocular dominance plasticity, reduced perineuronal net intensity and number, and changed their chemical composition restoring permissive low chondroitin 4-O-sulfation levels characteristic of juvenile mice. Activated adult plasticity had the typical functional and proteomic signature of juvenile plasticity. Transcriptomic and proteomic studies indicated that miR-29a manipulation regulates the expression of plasticity factors acting at different cellular levels, from chromatin regulation to synaptic organization and extracellular matrix remodeling. Intriguingly, the projection of miR-29a regulated gene dataset onto cell-specific transcriptomes revealed that parvalbumin-positive interneurons and oligodendrocytes were the most affected cells. Overall, miR29a is a master regulator of the age-dependent plasticity brakes promoting stability of visual cortical circuits.

INTRODUCTION

Brain postnatal development is characterized by temporal windows of high plasticity called critical or sensitive periods. The cellular mechanisms delimiting critical periods (CPs) have been classically studied using the model of ocular dominance (OD) plasticity of the visual cortex. Historical thinking was that OD plasticity is passively reduced with age; however it is becoming clear that plasticity levels are set by the integrated action of age- and experience-dependent factors actively promoting or suppressing circuit plasticity ("plasticity brakes") (Hensch and Quinlan 2018; Levelt and Hübener 2012). These factors can act at different cellular levels, from transcriptional and translational control to synaptic intracellular and extracellular environment. For instance, perineuronal nets (PNNs) enwrapping parvalbumin-positive (PV+) neurons increase in number and density, and change their chemical composition, with age inhibiting OD plasticity in the adult visual cortex (Carulli et al. 2010; Pizzorusso et al. 2002; Rowlands et al. 2018; Beurdeley et al. 2012; Miyata et al. 2012). Epigenetic factors such as histone acetylation and DNA methylation are also changed in coincidence with the closure of the critical period (CP) (Stroud et al. 2017; Tognini et al. 2015; Putignano et al. 2007), and their manipulation can reactivate juvenile-like plasticity in the adult (Putignano et al. 2007; Silingardi et al. 2010; Apulei et al. 2019). However, the mechanisms coordinating the expression of these plasticity mechanisms are totally unexplored.

MicroRNAs (miRNAs) are small molecules of non-coding RNA that regulate their targets by repressing mRNA translation and reducing mRNA stability (Bartel 2018). Because each miRNA can target several transcripts, miRNAs can efficiently coordinate different cellular pathways acting as master regulators of complex biologically processes (Rajman and Schratt 2017; Lippi et al. 2016). We hypothesized that this property of miRNAs could also mediate the coordinated age-regulation of different plasticity mechanisms setting CP timing. Previous work showed that during postnatal development there is a dramatic change of mouse visual cortex transcriptome accompanied by conspicuous changes in miRNA expression (Mazziotti et al. 2017). In particular, the most upregulated miRNA was miR-29a-3p (miR-29a), a member of a family including miR-29a, b1, b2, and c. Mir-29 family is strongly regulated by age

across different species and different tissues (Baumgart et al. 2012; Somel et al. 2010; Takahashi et al. 2012; Fenn et al. 2013; Nolan et al. 2014; Ugalde et al. 2011; Inukai et al. 2012). Its predicted targets are enriched in remodelling enzymes of extracellular matrix and epigenetic factors (Amodio et al. 2015; Fabbri et al. 2007; Foscarin et al. 2017), two classes of molecules regulating the CP for OD plasticity. Thus, we studied whether miR-29a could act as an age-dependent regulator of plasticity in the visual cortex.

Our results shows that miR-29a levels in the visual cortex are a critical determinant of plasticity acting on PNNs and epigenetic factors. Indeed, if miR-29a action is enhanced in juvenile mice, OD plasticity is blocked and PNNs are increased. Conversely antagonizing miR-29a in the adult promotes OD plasticity mechanisms sharing molecular and functional signature of juvenile plasticity. These effects are associated with the induction of plasticity factors acting on the chromatin epigenetic status and reestablishing immature PNNs. Thus, miR-29a is a master regulator of plasticity brakes in the visual cortex.

RESULTS

miR-29a age-dependent increase controls extracellular matrix and gene transcription regulating factors

In order to unravel key miRNAs that regulate postnatal development of the visual cortex, we reanalyzed our dataset of coupled miRNA-seq and RNA-seq in the developing mouse visual cortex. This analysis compared two time points: postnatal day 10 (P10), immediately before eye opening and CP onset, and P28 when mouse cortex displays developed functional properties (Mazziotti et al. 2017). The miR-29 family, and in particular miR-29a-3p, was the microRNA with the largest age-dependent up-regulation. Importantly, we found a highly significant overrepresentation of miR-29a predicted targets among the genes downregulated with age (fig.1a, 1051 predicted targets by Targetscan, 5429 genes downregulated with age; 554 genes in the intersection, odds ratio 4.40; Fisher exact test, $p < 0.001$), but not among age upregulated genes (fig.1b, 4339 upregulated genes with age; 164 genes in the

intersection, odds ratio 0.93; Fisher exact test p=0.93). These data suggest that miR-29a contributes to the age-dependent repression of gene expression by destabilization of its target transcripts. To gain insights into the molecular consequences of miR-29a upregulation with age, we performed a gene ontology analysis of miR-29a putative targets enriched in downregulated genes using the DAVID analysis (Huang et al. 2009; Huang et al. 2009). We found a significant overrepresentation in the categories "extracellular matrix organization" and "gene expression (transcription)", including key genes such as MMPs and ADAMTS, and Dnmt3a, Dnmt3b, TDG, Tet1, Tet2, and Tet3, respectively (fig.1c). Both pathways are well known to regulate OD plasticity of visual cortex during CP and to promote plasticity in adult rodents after their manipulation (Carulli et al. 2010; Fawcett et al. 2019; Pizzorusso et al. 2006; Pizzorusso et al. 2002; Rowlands et al. 2018; Tognini et al. 2015; Apulei et al. 2019). To gain better temporal resolution of the age-dependent regulation of miR-29a expression in the visual cortex, we performed a RT-PCR analysis and observed a dramatic 30-fold increase in mir-29a levels beginning after P10 and reaching a plateau around P120, when OD plasticity is strongly reduced (fig.1d; n=3/4 for each age; one-way ANOVA, p<0.0001; post hoc Tukey's test: p10 vs p25, p35, p60, p120, p200 p<0.0001; p25 vs p35, p60, p120, p200 p<0.0001; p35 vs p60, p120, p200, p<0.0001; other tests not significant). In parallel, we analyzed the age-dependent expression of Dnmt3a, a canonical and well-validated target of miR-29 (Amodio et al. 2015; Morita et al. 2013; Kuc et al. 2017; Fabbri et al. 2007). Dnmt3a expression was strongly downregulated with age (fig.1e; n=3/4 for each age; one-way ANOVA, p<0.0001; post hoc Tukey's test: p10 vs p25, p<0.0001; p10 vs p35, p<0.0001; p10 vs p60, p<0.0001; p10 vs p120, p<0.0001; p10 vs p200, p<0.0001; p25 vs p35, ns; p25 vs p60, ns; p25 vs p120, p<0.01; p25 vs p200, p<0.0001; p35 vs p60, p<0.0001; p35 vs p120, p<0.05; p35 vs p200, ns; p60 vs p120, ns; p60 vs p200, ns; p120 vs p200, ns), and, as shown in fig.1f, its levels were negatively correlated with miR-29a expression (Pearson correlation: r=-0.817, p<0.001). To investigate the distribution of miR-29a in visual cortical cells we performed *in situ* hybridization at P25 and P120 using LNA probes recognizing the mature miRNA. The results confirmed the strong age-dependent upregulation of miR-29a (fig.1g, N=3). Furthermore, at both ages the vast majority of cortical cells expressed miR-29a. Considering the importance of PV+ interneurons in

CP regulation (Takesian and Hensch 2013; Levelt and Hübener 2012), we specifically assessed miR-29a expression in these cells by triple staining for miR-29a, PV, and a nuclear marker (fig.1h). We found that miR-29a was expressed in many, if not all, PV+ interneurons.

Several molecular mediators of visual cortical plasticity, such as miR-132, Arc, Bdnf and Npas4, show experience-dependent expression (Tognini et al. 2015; Kim et al. 2018; Klein et al. 2007; Tognini et al. 2011; Gao et al. 2010). Thus, we investigated the effects of sensory stimulation on miR-29a expression by four different protocols of visual manipulation: i) dark rearing from birth (fig.2a; normal rearing (NR) (N=5) vs dark rearing (DR) (N=5); t-test, p=0.19); ii) DR from P10 (fig.2b; NR vs DR, N=4-5; t-test, p=0.70); iii) one week in darkness (P30-P37) followed by 4 h of light exposure (fig.2c; controls animals (ctr) vs one week of dark and no light re-exposure (0H) vs one week of dark and 4 hours of light re-exposure (4H), N=4 for each group; one-way ANOVA, p=0.68); and iv) 3 days of MD (P25-P28) (fig.2d; contralateral cortex (contra ctx) vs ipsilateral cortex (ipsi ctx) to deprived eye, N=9; paired t test, p=0.52). None of these manipulations affected miR-29a expression, indicating that expression of miR-29a is dictated by an intrinsic developmental timing that is not influenced by visual experience.

Taken together, these results show that miR-29a expression in the visual cortex is strongly age-dependent and correlates with the plasticity reduction occurring at the end of the CP, naturally leading to the hypothesis that miR-29a is causally linked to the age-dependent regulation of experience-dependent plasticity in visual cortical circuits.

Increasing miR-29a action during the CP blocks OD plasticity

If our hypothesis is correct, a premature increase of miR-29a during CP should be sufficient to reduce plasticity mimicking CP closure. To test this possibility, we induced a miR-29a upregulation during CP through intracortical administration of a synthetic miR-29a mimic (mim29a) and tested for the presence of OD plasticity (fig.3a). P24 mice were acutely injected with mim29a at three cortical sites surrounding the binocular visual cortex as identified by optical imaging of the intrinsic signal (IOS). Baseline visual responses were acquired 24h after injection and the eyelids of the eye

contralateral to the treated cortex were sutured shut. A second injection was performed at P26 and OD assessment and molecular analyses were performed at P28. An oligonucleotide with a scrambled sequence matching miR-29a nucleotide composition was injected as control.

To quantify the molecular efficacy of mim29a treatment, we measured the levels of miR-29a and of its validated target Dnmt3a at P28 (N=3) by RT-PCR. We detected nearly a doubling in miR-29a levels [fig.3b animals treated with scrambled mimic (scr) vs animals treated with miR-29a mimic (mim29a); t-test , p=0.005] and a corresponding significant decrease of Dnmt3a levels in the visual cortex treated with miR-29a mimic with respect to control-treated cortex (fig.3c scr vs mim29a t-test , p<0.0001).

We then assessed OD plasticity by recording IOS elicited by stimulation of either eye twice: before monocular deprivation (MD) at P24 and at the end of the protocol (P28). In control-treated mice, MD resulted in a reduction of the IOS elicited by stimulation of the contralateral eye. In mice treated with mim29a, this shift of OD was not observed (fig.3d; OD index (ODI) of scrambled treated mice (scr) (N=6) vs mim29a treated mice (mimic 29a) (N=8); two-way ANOVA RM, treatment X time, p= 0.029; post hoc Sidak's comparison, pre-MD scr vs post-MD scr, p=0.0009; pre-MD mimic 29a vs post-MD mimic 29a, p=0.21). The loss of plasticity induced by miR-29a mimic was confirmed by analysis of the molecular markers *Npas4* and *Bdnf* exon IV. Expression of these activity-dependent transcripts is reduced by monocular deprivation (Tognini et al. 2015). However, the amplitude of their down-regulation was smaller in miR-29a treated mice with respect to controls (fig.3e; scr vs mimic 29a; N=4; t-test, Npas4: p=0.038; Bdnf exIV: p=0.049).

Overall, these data demonstrate that precocious upregulation of miR-29a is sufficient to induce closure of the CP.

MiR-29a antagonization in adult mice promotes OD plasticity

We then tested whether antagonization of miR-29a in the adult (P>120) visual cortex could enhance OD plasticity. To reduce miR-29a biological activity in the visual cortex, we injected a locked nucleic acid (LNA) sequence complementary to miR29a (amiR-29a) or a control LNA oligonucleotide carrying a scrambled sequence. LNA

oligonucleotides stably bind their complementary miRNA thereby blocking its activity; moreover they are resistant to enzymatic degradation and are approved for use in humans (Khvorova and Watts 2017; Braasch and Corey 2001; Smith et al. 2019). Injections were performed at three sites surrounding the binocular visual cortex identified by IOS imaging. Molecular analyses were performed seven days after amiR-29a injections (fig.4a).

To assess the efficacy and the specificity of the amiR-29a treatment, we performed RT-PCR and RNA-seq analysis from the treated cortex. RT-PCR analysis revealed that amiR-29a treatment caused a decrease of mir-29a and an increase in the miR-29a target Dnmt3a (fig.4b-c; scr vs amiR-29a; N=3; t-test, miR-29a p=0.0010; Dnmt3a p=0.0019). RNA-seq detected expression of 15303 genes, out of which 1421 were differentially expressed genes (DEGs) between amiR-29a and control treated mice (q<0.05), with 985 showing up-regulation and 436 down-regulation (fig.4d; Suppl. table 1). Importantly, upregulated genes were significantly enriched in miR29a targets, but not in targets of other miRNAs (miTEA-miRNA Target Enrichment Analysis, p<0.001) (Steinfeld et al. 2013; Eden et al. 2009). Moreover, 26% of the upregulated genes were also downregulated by age suggesting that miR-29a inhibition could reverse part of the age-dependent transcriptional regulation. To assess amiR-29a effects at protein level, we performed proteomic analysis by means mass-spectroscopy-based proteomics with tandem-mass-tag (TMT) multiplexing in an independent set of animals. First, hierarchical clustering analysis of samples based of protein abundance showed that animals treated with amiR-29a cluster together demonstrating that the treatment has a coherent effect on global protein composition in the treated mice (Suppl. fig. 1). Among the 4595 detected proteins, we found 360 proteins to be significantly upregulated and 338 proteins to be significantly downregulated (Suppl. table 2). The fold changes of differentially expressed proteins and transcripts showed significant correlation (fig.4e, Spearman coefficient correlation, r=0.1218; p=0.008, suppl. table 3). Gene ontology analysis of positively correlated proteins and RNA performed with DAVID demonstrated an overrepresentation of extracellular matrix remodelers (fig.4f). Regulation of transcripts belonging to the two categories overrepresented among the predicted targets of miR-29a, i.e. extracellular matrix remodelers and epigenetic regulation of transcription, was also studied by RT-PCR.

We found a significant increase in MMP2, MMP9 and MMP13 (fig.4g; scr vs amiR-29a; N=4/8; t-test, MMP2: p<0.0001; MMP9: p=0.0015; MMP13: p=0.0005) as well as in Dnmt3a, Tet3, Gadd45a and Gadd45b (fig.4g; scr vs miR-29a; N=4/8; unpaired t test, Dnmt3a: p<0.0001; Tet3: p=0.008; Gadd45a: p=0.015; Gadd45b: p=0.012). In addition, the increase in the canonical miR-29a target Dnmt3a was also confirmed by western blot (fig.4i, scr vs miR-29a; N=7; t-test, DNMT3a: p=0.008). Intriguingly, all these factors have also been involved in the regulation of OD plasticity (Tognini et al. 2015; Apulei et al. 2019; Murase et al. 2017; Spolidoro et al. 2012; Kelly et al. 2015), suggesting that the age-dependent increase of miR-29a could contribute to repress plasticity by a coordinated downregulation of these permissive factors.

To get insights into cell specificity of amiR-29a effects, we projected regulated proteins on the cell clusters obtained by single-cell RNA seq of the adult mouse visual cortex (Tasic et al. 2016) (suppl. fig.2a) using the single cell portal for brain research launched by the Broad Institute of MIT. This approach visualizes the density of regulated proteins in the different cell subtypes. We observed an apparent enrichment of upregulated proteins in mature oligodendrocytes (suppl. fig.2b). This result is particularly interesting in light of the repressive role that myelin exerts on neuronal plasticity (McGee et al. 2005). Intriguingly, the top cell type enriched in downregulated proteins was the CP regulator class of PV+ cells (suppl. fig.2c). A high sensitivity of PV+ cells to miR-29a antagonization was also confirmed by immunohistochemistry analysis of PV intensity (suppl. fig.2d). The results show a shift in PV immunolabeling intensity towards low levels in the amiR-29a treated visual cortex treated (suppl. fig.2e), while PV+ cell density remained unaffected (suppl. fig.2f). This result suggests that miR-29a could be involved in maturation of PV cells and closure and the critical period.

Thus, we next asked whether miR-29a inhibition could promote OD plasticity in the adult. Mice were injected with amiR-29a or control at P120, 3 days later MD of the eye contralateral to the treated cortex was performed. After 4 days molecular and functional assessment was performed (scheme in fig.4a). Functional studies were done assessing the cortical response to the visual stimulation of the deprived and the nondeprived eye by visual evoked potentials (VEPs) recordings and IOS imaging. VEPs showed a significant reduction of the ratio between the response to the deprived and the nondeprived eye in mouse treated with amiR-29a LNA, but not in controls

(fig.5a; three groups of mice: non MD treated with saline (sal noMD), scramble treated MD (scr+MD), amiR29a treated MD (amiR-29a+MD) N=6/7; one-way ANOVA, p=0.0003; post hoc Tukey's test: sal noMD vs scr+MD, ns; sal noMD vs amiR-29a+MD, p=0.0002; scr+MD vs amiR-29a+MD, p=0.0169). IOS analysis confirmed the presence of OD plasticity in amiR-29a treated mice, but also extended these data showing that no difference in visual responses of amiR-29a and control mice were present before MD. AmiR-29a treated mice, but not control mice, showed a decline in the OD index after MD (fig.5b; ODI scr (N=5) vs amiR-29a (N=6), two-way ANOVA RM, treatment X time, p= 0.0074; post hoc Sidak's test, pre-MD scr vs post-MD scr, ns; pre-MD vs post-MD amiR-29a, p=0.0005). Thus, both VEPs and IOS performed in separate cohorts of mice confirmed activation of OD plasticity in adult mice by miR-29a inhibition.

Common functional and molecular signatures of MD during CP and after plasticity activation by miR-29a inhibition

Previous work suggested that short MD durations in juvenile mice result in selective depression of deprived eye responses (Sato and Stryker 2008; Frenkel and Bear 2004). Thus, we investigated whether this property is present also in the adult OD plasticity elicited by amiR-29a. Longitudinal assessment using IOS allows to analyze the absolute value of visual responses of each eye before and after MD. We found that MD significantly decreased the amplitude of visual responses of the deprived eye exclusively in amiR-29a treated mice but not in controls (fig.5c,d; amiR-29a (N=6) vs scr (N=5); two-way ANOVA RM, time X treatment interaction p=0.034; post hoc Sidak's test; pre-MD vs post-MD scr, ns; pre-MD vs post-MD amiR-29a, p=0.0008). As expected, the response amplitude of the ipsilateral nondeprived eye did not change in amiR-29a or control groups (fig.5c,e; amiR-29a (N=6) vs scr (N=5); two-way ANOVA RM, time X treatment interaction, ns).

Since amiR-29a induced plasticity shared functional characteristics with CP plasticity, we investigated whether plasticity induced in the adult visual cortex by miR-29a antagonization also displayed a molecular regulation typical of CP plasticity. We initially studied two activity-dependent genes (Npas4 and Bdnf exIV) strongly downregulated by MD during CP. We found that the effect of MD on their expression

was very pronounced in amiR-29a treated mice (fig.5f; scr vs amiR-29a; t-test; N=8-9, Npas4: p=0.035; N=4-5; Bdnf exIV: p=0.026). To achieve a more complete comparison of the molecular signature of amiR-29a induced plasticity with CP plasticity, we performed proteomic analyses comparing the changes induced by MD in young CP mice and in adult mice treated with amiR-29a (Suppl tables 4-5). In CP mice 2172 proteins were quantified. 168 proteins resulted to be significantly regulated by MD (p<0.05). The same analysis in adult mice treated with amiR-29a allowed the quantification of 1873 proteins, 199 of them significantly regulated by MD (p<0.05). To reveal whether a similar proteomic change was induced by MD in amiR-29a treated mice and in CP mice, we correlated the fold change expression induced by MD in the two datasets. All the measured proteins with a fold change>0.1 were included in the analysis. We found a positive correlation (fig.5g; Pearson correlation: r=0.193, p=0.019, Suppl. table 4) indicating a similar MD proteome signature in the two datasets. This protein group was further subdivided in two groups depending on showing correlation or anticorrelation between MD regulation during CP and after amiR-29a treatment. Then, we performed gene ontology analysis to characterize protein biological function. Due to the limited number of proteins we used the reactome platform. Intriguingly, while no specific enrichment was observed for the proteins showing inconsistent MD regulation, the proteins showing consisting MD regulation during CP and after adult treatment with amiR-29a were significantly enriched in categories such as CREB phosphorylation through the activation of CaMKII (R-MMU-442729), unblocking of NMDA receptor (R-MMU-438006), transmission across chemical synapses (R-MMU-112315) known to be involved in OD plasticity (fig.5h). Moreover, we analyzed consistently MD regulated proteins using SynGo, a new database specific for proteins whose involvement in synaptic functions and plasticity is well established (Koopmans et al. 2019). The results demonstrated that correlated MD regulated proteins were highly significantly enriched in presynaptic and postsynaptic proteins mostly located on excitatory synapses. No enrichment was observed for anticorrelated proteins (fig.5i,j). A full list of the significant categories is shown in Suppl. table 5,6. Thus, the mechanisms underlying OD plasticity induced by miR-29a antagonization in the adult visual cortex activates molecular processes similar to those activated during CP plasticity.

miR29a age-dependent expression regulates PNN structure and chemical composition

In order to understand the mechanisms by which different levels of miR-29a in adult and CP mice affect OD plasticity, we investigated PNN formation after manipulation of miR-29a levels in the visual cortex of juvenile and adult mice. Indeed studies in rodents showed that PV+ cell PNN maturation in the visual cortex closes the CP for OD plasticity (Carulli et al. 2010; Fawcett et al. 2019; Pizzorusso et al. 2006; Pizzorusso et al. 2002; Rowlands et al. 2018; Beurdeley et al. 2012; Lensjø et al. 2017; Boggio et al. 2019). Moreover, in silico prediction and our experimental evidences showed that miR-29a targets are enriched in extracellular remodelling factors, and that the PV+ cells show significant proteomic modulation by miR-29a (fig. 1c, fig. 4g, suppl. fig. 2c,d). Thus, we revealed PNNs using Wisteria Floribunda Agglutinin (WFA) both in juvenile mice treated with miR-29a mimic and in adult mice treated with amiR-29a.

We found that inducing the high miR-29a levels typical of the adult in the juvenile visual cortex by miR-29a mimic, resulted in enhanced PNN labelling (fig.6a-b, scr vs mim29a, N=3 mice per group; t-test, p=0.014), while no effects was observed on PNN density (fig.6a-c, scr vs mim29a, N=3 mice per group; t-test, p=0.20). Subdividing the distribution of PNN intensity in tertiles corresponding to strong, medium and faint PNNs, we observed a significantly higher fraction of strong PNNs in miR-29a mimic treated mice as compared to controls (fig.6 d-e; scr N=1438 cells vs mim29a N=1749 cells, Kolmogorov-Smirnov test, p value< 0,0001). A high fraction of strongly labelled PNNs is typical of adult mice expressing low OD plasticity levels (Fawcett et al. 2019). Thus, premature high levels of miR-29a resulted in PNN early maturation and reduced plasticity levels.

To test whether the age-dependent increase of miR-29a triggers PNN maturation and CP offset, we analysed PNNs in adult mice treated with amiR-29a. amiR-29a treatment resulted in a reduction in PNN intensity (fig. 6f-g; scr vs amiR-29a, N=3 mice per group; t-test, p=0.047) and density (fig. 6f-h; scr vs amiR-29a, N=3 mice per group; t-test, p=0.03), determining a lower fraction of strong PNNs (fig. 6i-j; scr N=1883 cells vs amiR-29a N=1937 cells, Kolmogorov-Smirnov test, p< 0.0001). Age-dependent PNN maturation also involves changes in glycosaminoglycan (GAG) sulfation of chondroitin

sulfate proteoglycans. Indeed, during PNN maturation there is a shift from GAG sulfation in 6 (C6S) position to sulfation in 4 (C4S) position. Previous work showed that restoring the juvenile form of GAG sulfation promotes plasticity in the adult visual cortex and renders CSPGs more permissive to axon growth, regeneration and plasticity (Miyata et al. 2012; Yang et al. 2017). Thus, we tested if amiR-29a could also affect mature PNNs also by reducing the adult C4S form of GAG sulfation. Biochemical analyses showed a significant decrease of C4S in adult animals treated with amiR-29a (fig. 6k; ng of C4S/ug normalized to untreated cortex for scr and amiR-29a mice; N=4-5, unpaired t test, p=0.0008) suggesting a reduction of the inhibitory role of PNNs for plasticity. C4S decrease was associated with a highly significant increase of ArsB (Zhang et al. 2014; Yoo et al. 2013), an enzyme that catalyzes C4S removal and that has been suggested to be a target of miR-29 family including miR-29a (fig. 6l; N=4, scr vs amiR-29a treated cortex, unpaired t test, p=0.043). Thus, inducing in the adult visual cortex the low levels of miR-29a typical of juvenile mice promotes OD plasticity and restores PNN condensation and chemical composition typical of juvenile highly plastic mice .

Discussion

Our work shows that miR-29a is a master age-dependent regulator of plasticity in the visual cortex. Indeed, we showed that manipulations of miR-29a action mimicking adult or juvenile levels of miR-29a correspondingly determine adult or juvenile levels of OD plasticity. Premature increase of miR-29a levels in young mice blocked juvenile OD plasticity while miR-29a downregulation in adult animals induced OD plasticity with the typical physiological and proteomic signature of juvenile plasticity.

To deeply characterize the molecular underpinnings of miR-29a action on OD plasticity, we performed transcriptomic and proteomic analyses after amiR-29a treatment in adult mice. The results showed a remarkable convergence of miR-29a action on plasticity brakes controlling plasticity levels by acting on different cell functions and compartments. For example, previous work showed that OD plasticity can be promoted in the visual cortex by inhibiting epigenetic enzymes decreasing histone acetylation such as HDACs, or activating DNA methylation regulatory

pathways involving Gadd45b/g and Tets (Silingardi et al. 2010; Putignano et al. 2007; Apulei et al. 2019). Importantly, the results of these interventions restore the strong and highly malleable epigenetic control of chromatin typical of juvenile animals (Stroud et al. 2017; Tognini et al. 2015; Putignano et al. 2007; Baroncelli et al. 2016; Vierci et al. 2016). Our analysis shows that miR-29a levels are tightly correlated with Dnmt3a, and that manipulation of miR-29a levels dramatically affects Dnmt3a; Tet1,2 and 3; and Gadd45a and b. Moreover, antagonization of miR-29a also resulted in induction of Arc, a gene capable of activating OD plasticity in the adult (Jenks et al. 2017; McCurry et al. 2010), and other plasticity factors such as Egr-1 and Egr-2, Nr4a1 and Nr4a2 (Mo et al. 2015; Chen et al. 2014; Knapska and Kaczmarek 2004;). Furthermore, our work shows that miR-29a level in the visual cortex is a critical determinant of PNN maturation, another important plasticity brake in the visual cortex (Carulli et al. 2010; Pizzorusso et al. 2006; Pizzorusso et al. 2002; Lensjø et al. 2017; Rowlands et al. 2018), and in other brain areas (Fawcett et al. 2019; Reichelt et al. 2019). PNNs are specialized extracellular matrix structures predominantly associated with PV interneurons in the visual cortex. They have essentially two structural roles: acting as scaffold for plasticity regulating the binding of molecules such as Otx2 (Spatazza et al. 2013; Beurdeley et al. 2012) and Sema3a (Boggio et al. 2019), and limiting new synaptic connections (Faini et al. 2018). Adult mice treated with amiR-29a strongly upregulate extracellular matrix remodelers like MMP2, MMP13, and MMP9 and reduce PNNs intensity and density, while young animals treated with miR-29a mimic show a premature increase of PNNs intensity. Mir-29a also regulated the age-related change in chemical composition of PNNs. Downregulation of miR-29a in adult mice causes a reduction of sulfonation of chondroitin sulfate in position 4 (C4S), a chemical modification of CSPGs typically enriched in adult brain and associated with reduced axon growth, regeneration and OD plasticity in the visual cortex (Yang et al. 2017; Miyata et al. 2012; Foscarin et al. 2017). This decrease is accompanied by upregulation of the miR-29a target ArsB (Bhattacharyya et al. 2015), the enzyme responsible to remove sulfate groups from C4S. Overall, these data indicate that miR-29a coordinates the age-dependent regulation of several molecular pathways regulating CP plasticity.

Importantly, miR-29a expression is not regulated by visual experience, suggesting that miR-29a mediate exclusively the action of age on CP timing. This information must be integrated with experience dependent signals unrelated to miR-29a, such as NARP and BDNF (Huang et al. 1999; Gu et al. 2013), to achieve input specific plasticity and experience-dependent regulation of CP timing. Mir-29a could act on CP timing also interacting with circadian clock mechanisms. Indeed previous work showed that clock mutation in PV cells causes an altered CP (Kobayashi et al. 2015), and miR-29a has been shown to affect circadian rhythmicity period through regulation of Per1 and 2 mRNA stability and translation (Chen et al. 2013).

Although mir-29a is broadly expressed in different cell types in the visual cortex, several data indicate that miR29a is a powerful molecular regulator of PV cell maturation. Our in situ hybridization and previous data obtained with Ago-CLIP (He et al. 2012) showed that PV cells express high levels of miR-29a. Furthermore, the time course of cortical miR-29a expression is correlated with the maturation of WFA positive PNNs enwrapping PV cells. Moreover, mimicking or antagonizing miR-29a correspondingly modulated PV cell PNNs. PV levels were also downregulated by miR-29a antagonization in adult animals, and bioinformatic analysis of proteomic data showed that PV cells represent the most affected cell population in terms of protein downregulation after amiR-29a treatment. Thus, PV cells could be preferential miR-29a targets mediating miR-29a action on CP timing.

Our results showing that miR-29a is a strong remodeler of PNNs open a therapeutic perspective for miR-29a and other miR-29 family members. Indeed, manipulations of PNNs, both PNN increases or decreases depending on the type of pathological condition, have been proposed for several diseases including schizophrenia, autism, addiction and seizures (Wen et al. 2018; Pantazopoulos and Berretta 2016; Sorg et al. 2016). For example, preclinical studies and the analysis of human post-mortem samples of schizophrenic patients showing reductions of aggrecan and WFA staining indicated that PNN alterations could be a key component of the physiopathology of psychiatric disorders (Pantazopoulos et al. 2015; Pantazopoulos et al. 2010). On the other hand, several works have demonstrated that reduction of PNNs can be used to promote plasticity during aging and recovery from brain lesions (Soleman et al. 2012; Gherardini et al. 2015; Hill et al. 2012; Wiersma et al. 2017; Fawcett et al. 2019).

Moreover, the miR-29 family is acutely neuroprotective in stroke models (Ouyang et al. 2013; Khanna et al. 2013; Kobayashi et al. 2019). Considering that antimirs and miRNA mimics are under clinical trials for different human pathological conditions (Rupaimoole and Slack 2017), modulation of miR-29 family levels could be a concrete possibility for many brain diseases.
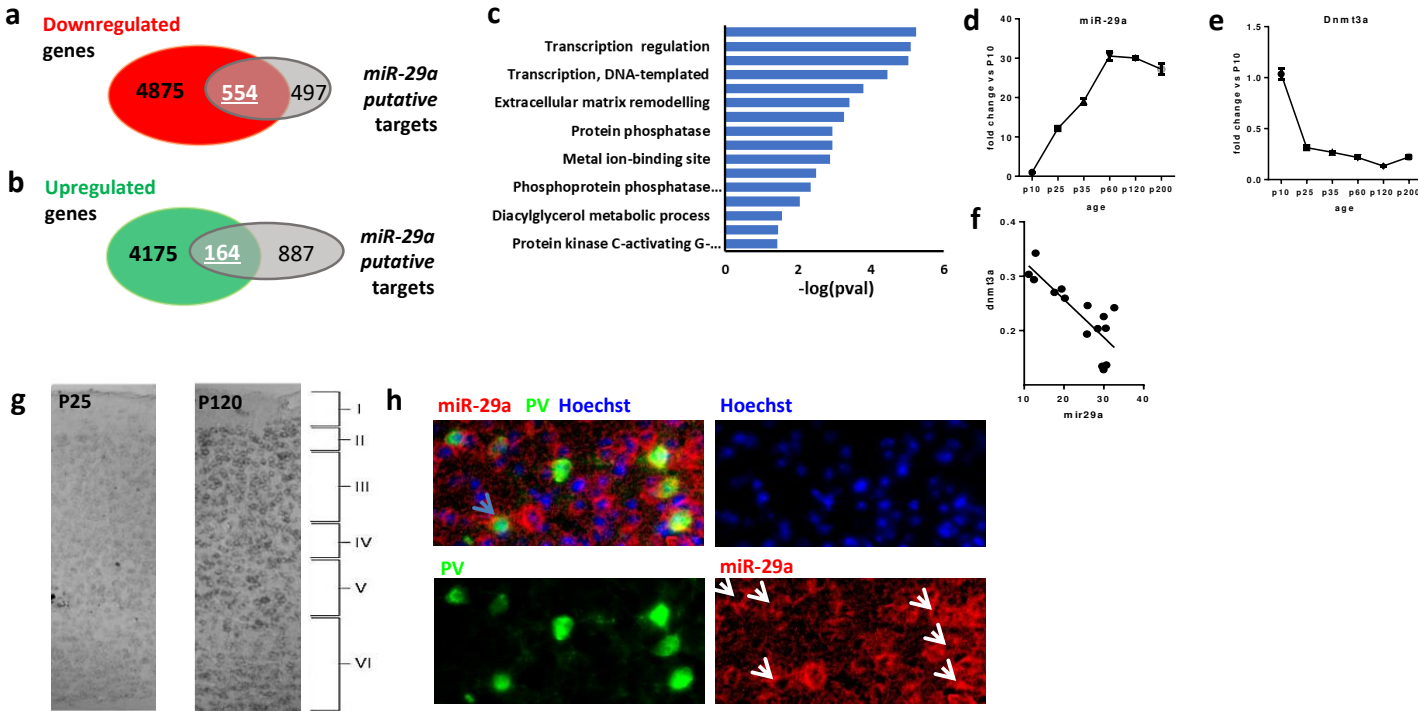
Fig.1

Figure 1: miR-29a age-dependent regulation coordinates expression of extracellular and epigenetic remodelling factors.

Venn diagram showing the intersection between putative miR-29a target genes and **a)** age-downregulated genes, and **b)** upregulated genes. **c)** DAVID functional annotation clustering analysis showing the most significant enriched pathways of putative targets enriched in downregulated genes. **d)** Mature miR-29a and **e)** Dnmt3a expression level (normalized to P10) at different ages. **f)** Scatter plot showing that miR-29a and Dnmt3a levels in the visual cortex display a strong negative correlation. Each circle represents data from a single animal. **g)** Representative example of *in situ* hybridization on visual cortex (left P25, right P120) using a LNA probe against miR-29a. Calibration bar 150 μm. **h)** Example of co-staining for PV (green), miR29 (red) and nuclear marker (blue). Calibration bar 15 μm. Error bars represent ±SEM. Asterisk statistical significance.
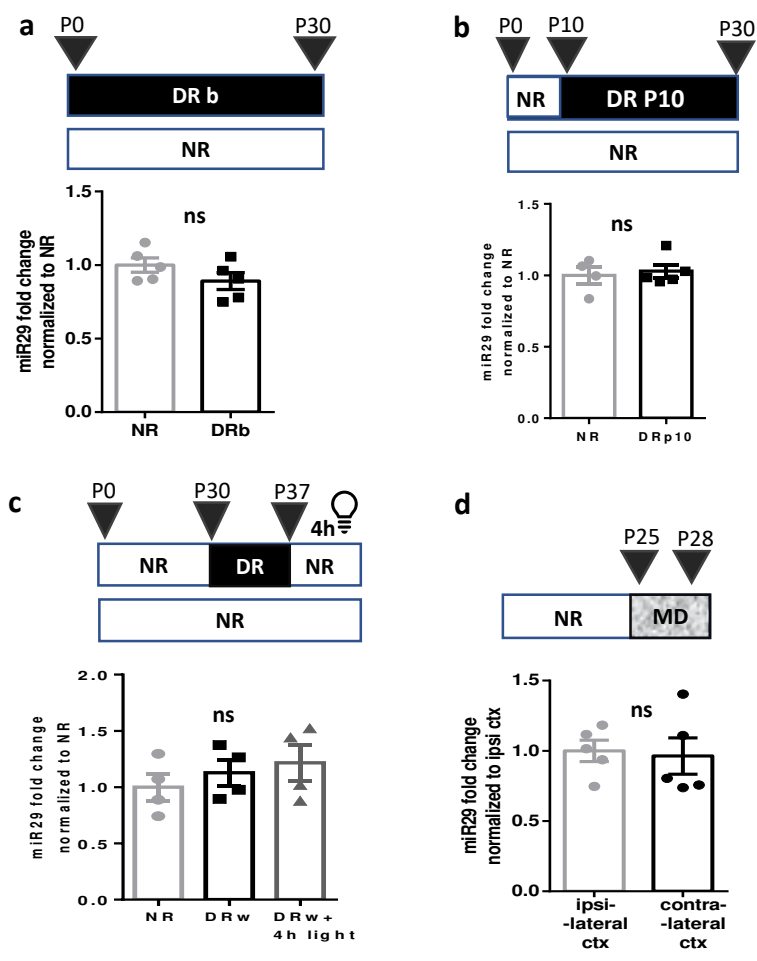
Fig.2

a

P0   P30

DR b

NR

ns

miR29 fold change normalized to NR

NR   DRb

b

P0   P10   P30

NR   DR P10

NR

ns

miR29 fold change normalized to NR

N R   D R p10

c

P0   P30   P37   4h

NR   DR   NR

NR

ns

miR29 fold change normalized to NR

N R   D R w   D R w + 4h light

d

P25   P28

NR   MD

ns

miR29 fold change normalized to ipsi ctx

ipsi-lateral ctx   contra-lateral ctx

Figure 2: miR-29a expression is not experience-dependent.

Mature miR-29a levels were not affected by dark rearing **a)** from birth (DRb) and **b)** from P10 (DRp10) with respect to normal rearing mice (NR). Analysis was performed at P25. **c)** Mature miR-29a levels were not affected by a one week period of dark rearing beginning at P30 (DRw) and by a subsequent exposure to light (DRw+4h) compared to NR mice. **d)** MD did not affect miR-29a expression in the visual cortex contralateral (contra ctx) to the deprived eye with respect to the ipsilateral cortex (ipsi ctx). Error bars represent ±SEM. Asterisk statistical significance.
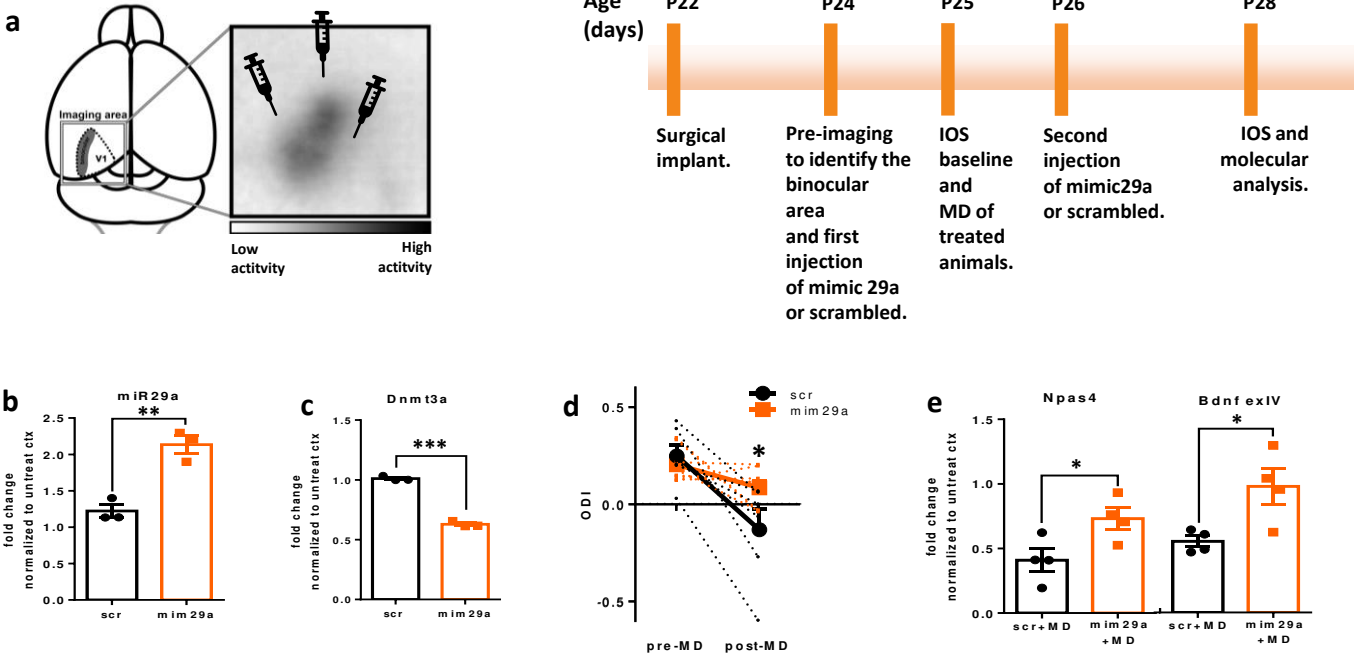
Fig.3

Figure 3: miR-29a upregulation blocks OD plasticity of young mice.

a) Experimental design for miR-29a mimic treatment in young mice. **b)** MiR-29a and **c)** Dnmt3a expression in the cortex treated with scrambled or miR-29a mimic. Data were normalized to the untreated cortex of the same animal. **d)** IOS analysis. Ocular dominance index (ODI) of deprived animals treated with scrambled (scr, black lines) and miR-29a mimic (mim29a, orange lines) before and after 3 days of MD. Dashed lines represent single animals, continuous lines the group average. **e)** The effects of MD on expression of Npas IV and Bdnf exIV is reported as ratio between expression level of deprived and nondeprived cortex for animals treated with scrambled (scr+MD) and miR-29a mimic (mim29a+MD). Each symbol represents the result of a single mouse. Error bars represent ±SEM. Asterisk statistical significance, *p<.05 **p<0.001

Fig.4
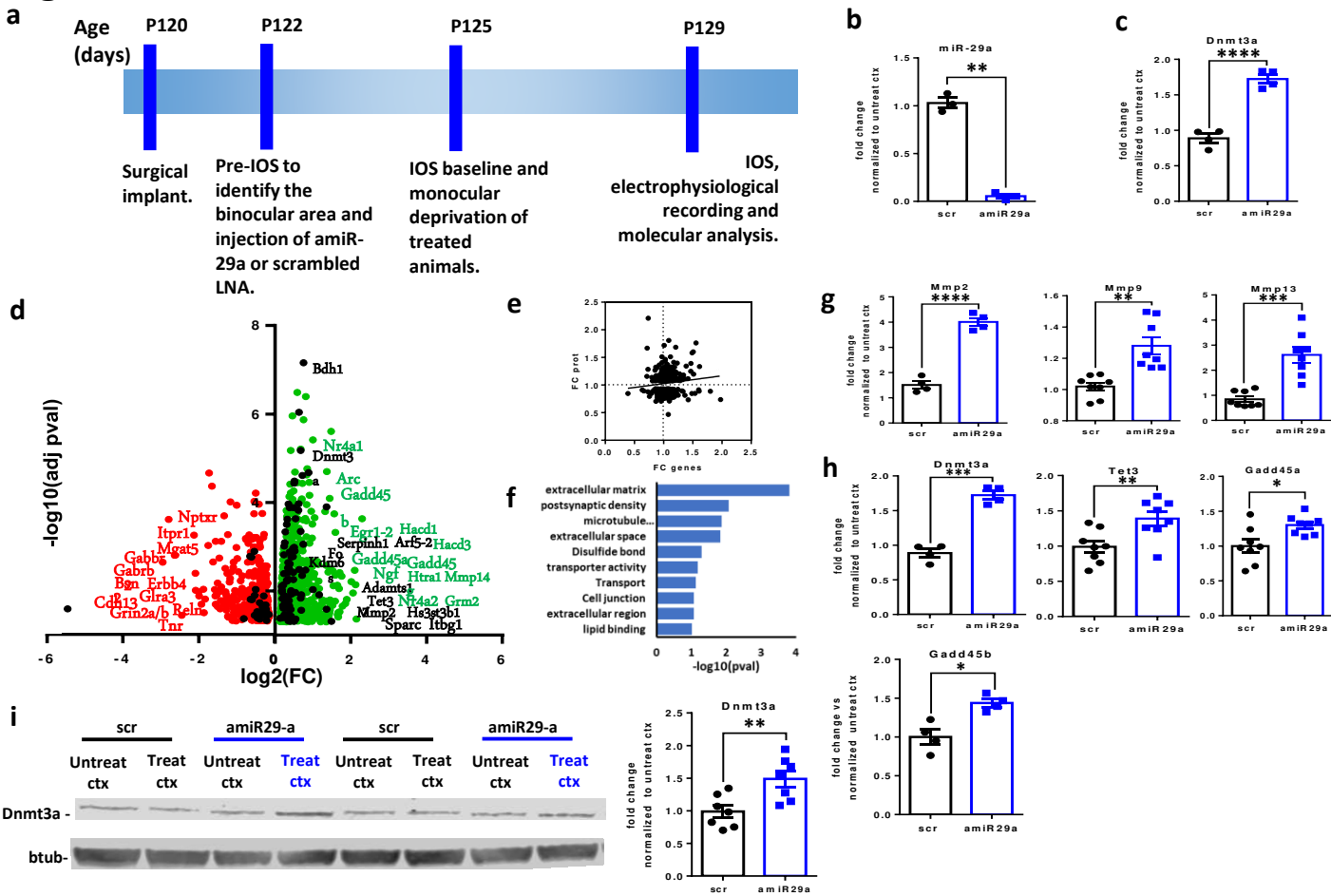
Figure 4: Transcriptomic and proteomic effects of miR-29a downregulation.

a) Experimental design for antimir-29a treatment in adult mice. **b)** MiR-29a and **c)** Dnmt3a expression are dramatically affected by amiR-29a. Fold change values with respect to the contralateral untreated cortex are reported for mice treated with amiR-29a or scrambled (scr). **d)** Volcano plot of RNA-seq analysis showing for each differentially expressed gene (scr versus amiR29a) the relationship between its fold change and statistical significance comparing the scr and amiR-29a treated cortex. Black circles represents putative targets of miR-29. **e)** Scatter plot correlating the expression changes induced by miR-29a antagonization in adult mice at proteomic and transcriptomic levels. Black line is the linear regression with 95% confidence band. **f)** DAVID functional annotation clustering analysis showing the most significant enriched pathways of genes and proteins positivity correlated. Error bars represent ±SEM. Asterisk statistical significance, **p<0.01 ****p<0.0001. **g**) RT-PCR analysis of the expression of extracellular matrix remodellers (MMP2,MMP9,MMP13) and **h**) epigenetic factors (Dnmt3a, Tet3, Gadd45a, Gadd45b) in animals treated with amiR-29a with respect to control animals treated with scrambled LNA (scr). Data for scr and amiR-29 treated cortices are normalized to the contralateral untreated cortex of the same animal. **i)** Dnmt3a upregulation is confirmed also by western blot analysis of visual cortex. Left: example of Dnmt3a western blot. The lanes corrisponding to the treated (treat scr or treat amiR-29a) and untreated (untreat scr or untreat amiR-29a) cortex (ctx) of two amiR-29a treated and two scr treated mice are reported. Right: quantification of the data shows Dnmt3a upregulation by amiR29a. The results are expressed as fold change normalized to untreated cortex. Each symbol represent the result of one animal. Error bars represent ±SEM. Asterisk statistical significance, **p<0.01, ***p<0.0001 ****p<0.0001.
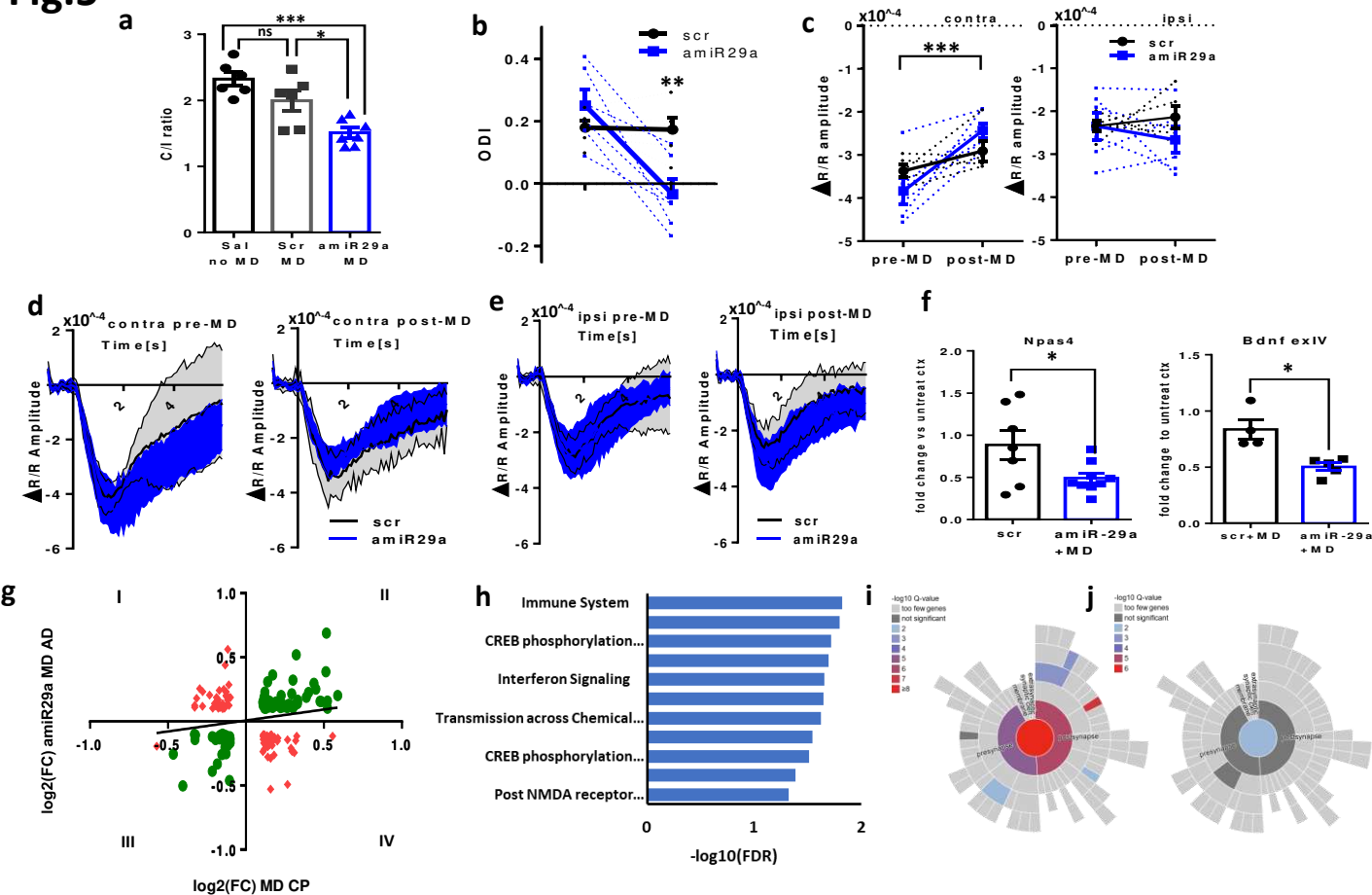
Fig.5

Figure 5: miR-29a downregulation restores experience-dependent plasticity in adult mice with similar physiological and proteomics features of juvenile mice.

a) VEPs analysis. Ratio between contralateral and ipsilateral eye responses (C/I ratio) in animal treated with saline and not deprived (sal no MD), with scrambled LNA and deprivation (scr MD), with antimir-29a LNA and deprivation (amiR29a MD). **b)** IOS analysis. ODI of deprived animals treated with scrambled (black lines) and antimiR-29a LNA (blue lines). Dashed lines connect pre- and post-MD ODI values of each animal. Full lines represent the group average. **c)** IOS amplitude in response to contralateral eye (contra) and ipsilateral eye (ipsi) stimulation. Other conventions as in b. **d)** Average time course of the IOS response to visual stimulation of the contralateral eye (contra) pre- and post-MD. Grey traces are scrambled animals; blue traces are amiR-29a animals. **e)** Same as in d for ipsilateral eye (ipsi) pre- and post-MD responses. (**f)** The effects of MD on Npas IV and Bdnf exIV expression is reported as the ratio between expression levels of deprived and nondeprived cortex for animals treated with scrambled (scr+MD) and amiR-29a (amiR-29a+MD). Each symbol represent the result of one animal. Error bars represent ±SEM. Asterisk statistical significance, **p<0.01, ***p<0.0001 ****p<0.0001. **g)** Scatter plot correlating the expression changes induced by MD in young mice (MD CP, x-axis) with the effects observed in the adult deprived mice treated with amiR-29a (amiR29a MD AD, y-axis). Proteins present in both data sets and showing an expression fold change (FC>0.1) are reported. Green symbols represent positively correlated proteins; red symbols report anticorrelated proteins. **h)** Reactome analysis of positively correlated proteins showing enrichment in gene categories related to synaptic plasticity. For each category the fold enrichment in positively correlated proteins is reported as function of statistical significance (-log10 FDR of differentially expression). **c)** Hierchical dendrograms of synaptic proteins (synGO database) showing significant enrichment by colour-code. Several highly significant categories are present for positively correlated proteins. **i)** A weak significance only for the general "synaptic proteins" categories is present the anticorrelated protein set.
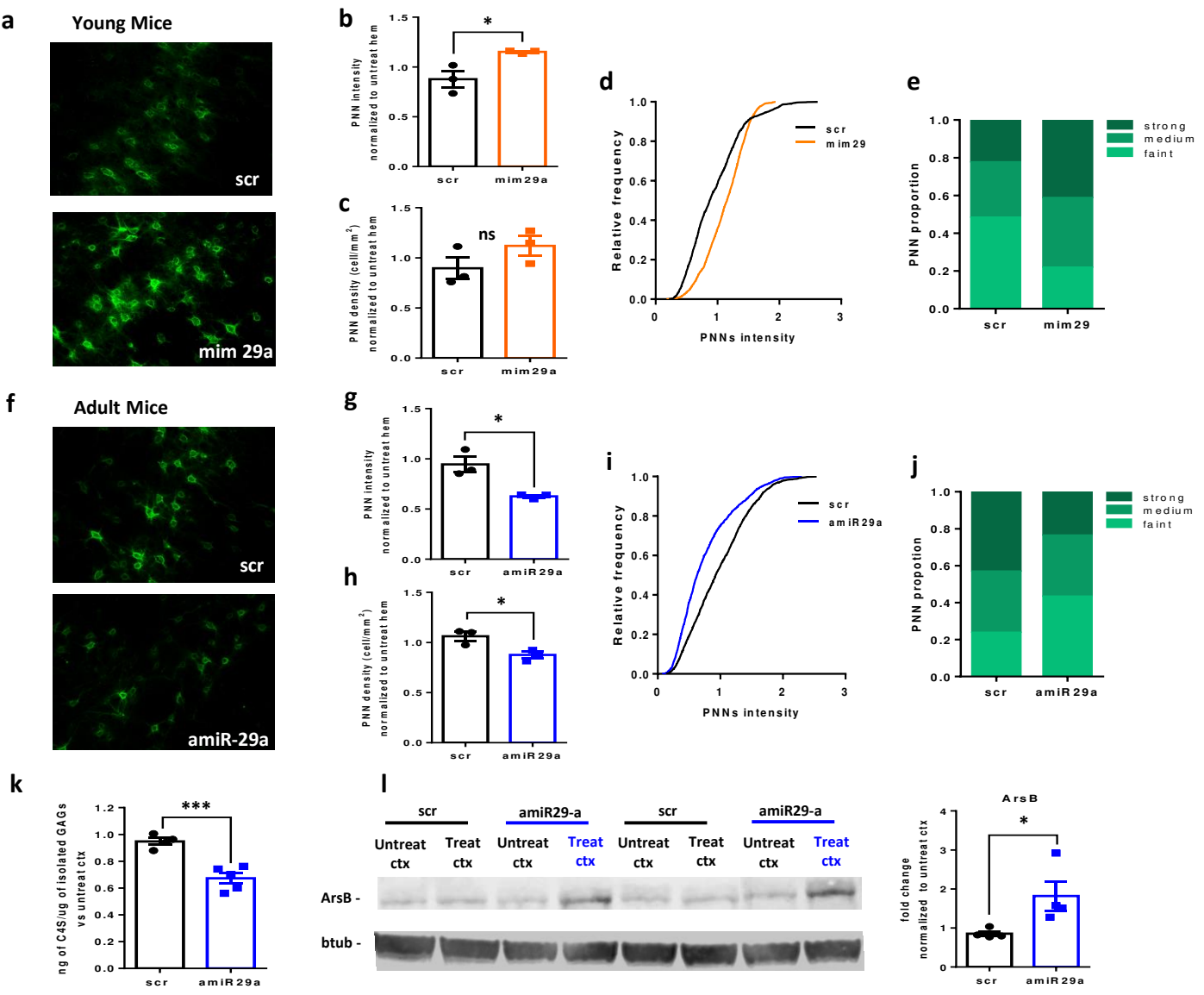
Fig.6

Figure 6: Manipulations of miR-29a levels promote changes in PNNs

a) Images of WFA-labeled PNNs of scrambled treated visual cortex (top) and miR-29a mimic (bottom) in young mice. Calibration bar 60 μm. **b)** Quantification of PNN intensity and **c)** density for each animal. **d)** Cumulative frequency of PNNs intensity in scrambled and mimic treated young mice expressed as cumulative frequency. **e)** PNN distribution in classes of intensity in mice treated with scrambled and mimic 29a.**f**) Images of WFA-labeled PNNs of scrambled treated visual cortex (top) and amiR-29a LNA (bottom) in adult mice. Calibration bar 60 μm. **g)** Quantification of PNN intensity and **h)** density for each animal. **i)** Cumulative frequency of PNNs intensity in scrambled and amiR29a treated adult mice. **j)** PNN distribution in classes of intensity in mice treated with scrambled and amiR29a. **k)** Biochemical quantification of C4S in adult amiR-29a treated mice as compared to scrambled animals**. l)** Example of Arylsulfatase B (ArsB) western blot. Top: The lanes corrisponding to the treated (treat scr or treat amiR-29a) and untreated (untreat scr or untreat amiR-29a) cortex (ctx) of two amiR-29a treated and two scr treated mice are reported. Bottom: quantification of the data shows ArsB upregulation by amiR29a. The results are expressed as fold change normalized to untreated cortex. Each symbol represent the result of one animal. Error bars represent ±SEM. Asterisk statistical significance, *p<.05 **p<0.001
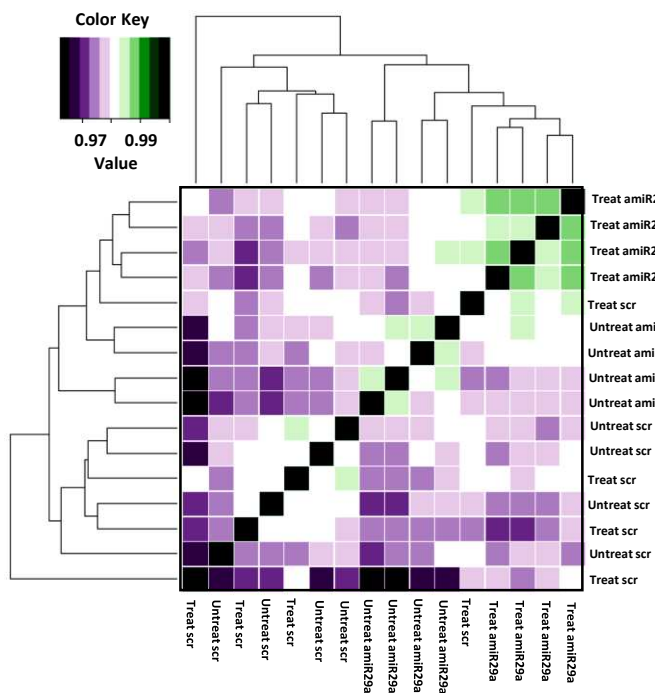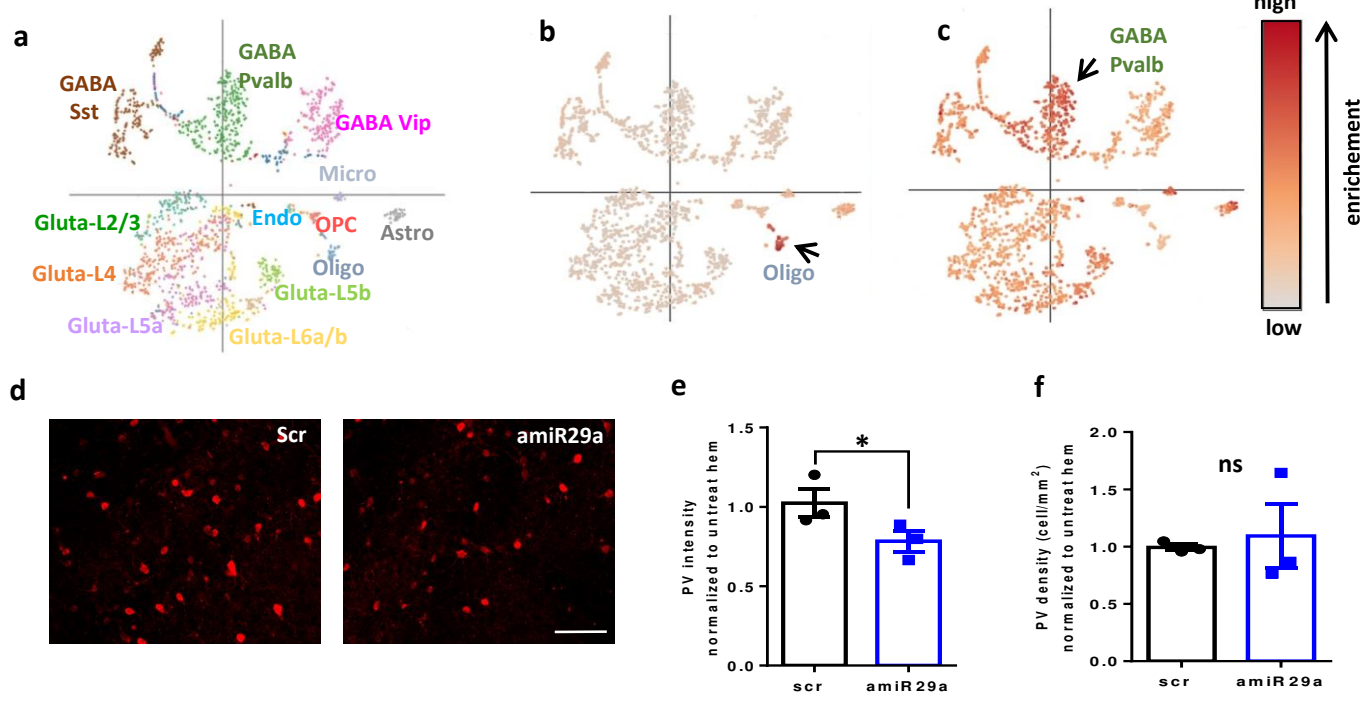
Suppl. Fig.1

Suppl Figure 1: Proteomic modulations induced by miR-29a downregulation.

Hierarchical clustering graph of proteomic results showed that animals treated with amiR-29a LNA clustering together (green squares)

Suppl. Fig.2

Suppl. Figure 2: Single cells analysis.

a) Single-cell clusters of genes expressed in adult visual cortex from Tasic et al 2016. **b)** In silico single cell analysis of amiR-29a upregulated and **c)** downregulated proteins. The most affected cell populations are, respectively, mature oligodendrocytes and "GABA parvalbumin" cluster cells. **d)** Examples of PV immunostaining in adult mice treated with scrambled (right) and amiR-29a LNA (left). Calibration bar 100 µm. **e)** Quantification of PV intensity and **f)** density per each animal. Error bars represent ±SEM. Asterisk statistical significance.